doi:10.1093/brain/aws296 Brain 2012: 135; 3635–3644 | 3635

BRAIN
A JOURNAL OF NEUROLOGY

Abnormal thalamocortical structural and functional connectivity in juvenile myoclonic epilepsy

Jonathan O'Muircheartaigh,[1,2] Christian Vollmar,[3,4,5] Gareth J. Barker,[1] Veena Kumari,[6] Mark R. Symms,[3,5] Pam Thompson,[3,5] John S. Duncan,[3,5] Matthias J. Koepp[3,5] and Mark P. Richardson[7]

1 Department of Neuroimaging, King's College London, Institute of Psychiatry, London SE5 8AF, UK
2 Department of Engineering, Brown University, Providence, RI 02912, USA
3 Department of Clinical and Experimental Epilepsy, Institute of Neurology, University College London, London, WC1N 3BG, UK
4 Department of Neurology, Epilepsy Centre, University of Munich, Munich 81377, Germany
5 Epilepsy Society, MRI Unit, Chalfont St Peter SL9 0RJ, UK
6 Department of Psychology, King's College London, Institute of Psychiatry, London SE5 8AF, UK
7 Department of Clinical Neuroscience, King's College London, Institute of Psychiatry, London SE5 8AF, UK

Correspondence to: Mark P. Richardson
Department of Clinical Neuroscience,
King's College London, Institute of Psychiatry,
Box P043, De Crespigny Park,
London SE5 8AF, UK
E-mail: Mark.Richardson@kcl.ac.uk

Juvenile myoclonic epilepsy is the most common idiopathic generalized epilepsy, characterized by frequent myoclonic jerks, generalized tonic-clonic seizures and, less commonly, absences. Neuropsychological and, less consistently, anatomical studies have indicated frontal lobe dysfunction in the disease. Given its presumed thalamo–cortical basis, we investigated thalamo–cortical structural connectivity, as measured by diffusion tensor imaging, in a cohort of 28 participants with juvenile myoclonic epilepsy and detected changes in an anterior thalamo–cortical bundle compared with healthy control subjects. We then investigated task-modulated functional connectivity from the anterior thalamic region identified using functional magnetic resonance imaging in a task consistently shown to be impaired in this group, phonemic verbal fluency. We demonstrate an alteration in task-modulated connectivity in a region of frontal cortex directly connected to the thalamus via the same anatomical bundle, and overlapping with the supplementary motor area. Further, we show that the degree of abnormal connectivity is related to disease severity in those with active seizures. By integrating methods examining structural and effective interregional connectivity, these results provide convincing evidence for abnormalities in a specific thalamo–cortical circuit, with reduced structural and task-induced functional connectivity, which may underlie the functional abnormalities in this idiopathic epilepsy.

Keywords: juvenile myoclonic epilepsy; connectivity; functional MRI; diffusion MRI
Abbreviations: DTI = diffusion tensor imaging; SMA = supplementary motor area

Introduction

Juvenile myoclonic epilepsy is a common subtype of idiopathic generalized epilepsy (Janz, 1985), characterized by myoclonic jerks, generalized tonic-clonic seizures and, less commonly, absences (Genton and Gelisse, 2001). The pathogenesis of idiopathic generalized epilepsy is unclear, but the characteristic generalized spike and wave discharges implicate thalamo–cortical

Received June 13, 2012. Revised August 18, 2012. Accepted September 11, 2012

interactions (Blumenfeld, 2003). In animal models of this group of diseases, abnormal activity in both thalamic and cortical structures is needed for generalized spike and wave generation (e.g. Danober *et al.*, 1998). EEG emphasis during generalized spikes and waves is often strongest in frontal regions (Montalenti *et al.*, 2001).

Cognitively, frontal dysexecutive, verbal and attentional neuropsychological impairments have been reported in juvenile myoclonic epilepsy. However, in addition to direct cortical effects, such frontal executive changes can also occur as a function of subcortical damage (Krause *et al.*, 2012), via the disruption of striato–thalamo–frontal circuits (Alexander and Crutcher, 1990). Subcortical structural alterations have been reported in idiopathic generalized epilepsies (Du *et al.*, 2011) and juvenile myoclonic epilepsy specifically (Deppe *et al.*, 2008; Keller *et al.*, 2011). Thus, although frontal cognitive dysfunction is commonly linked to subtle focal cortical abnormalities (e.g. Betting *et al.*, 2006; Kim *et al.*, 2007; O'Muircheartaigh *et al.*, 2011*a*; Vollmar *et al.*, 2011), epilepsy is a pathology of functional networks (Blumenfeld, 2003), and subcortical integrity is critical for normal cortical network function.

Simultaneous EEG–functional MRI studies in idiopathic generalized epilepsy have consistently demonstrated distributed networks of activity in cortical and subcortical regions, especially the thalamus, correlating to spike-and-wave activity (Aghakhani *et al.*, 2004; Gotman *et al.*, 2005; Hamandi *et al.*, 2006). We have previously demonstrated cortico-cortical structural connectivity changes between supplementary motor area (SMA) and motor cortex in juvenile myoclonic epilepsy (Vuillemoz *et al.*, 2010; Vollmar *et al.*, 2011, 2012); these were linked to cognitive effort during a working memory task, implicating a dysfunction in cognition-linked motor control. Further analysis, using diffusion tensor imaging (DTI)-based connectivity fingerprinting and clustering techniques, showed altered connectivity of the SMA to various cortical areas and descending motor pathways, consistent with clinical observations in juvenile myoclonic epilepsy.

Here we focus on thalamo–cortical connectivity; firstly, we investigate DTI tractography-defined thalamo–cortical bundles, using a novel method of segmenting tractography patterns (O'Muircheartaigh *et al.*, 2011*b*) that allows a comparison of a structural connectivity metric between patients with juvenile myoclonic epilepsy and healthy controls. Using the results of the DTI analysis, we then investigate altered thalamo–cortical functional connectivity during phonemic verbal fluency, a task impaired in participants with juvenile myoclonic epilepsy (Kim *et al.*, 2007; Roebling *et al.*, 2009; O'Muircheartaigh *et al.*, 2011*a*) and which may induce myoclonic jerks (da Silva Sousa *et al.*, 2005).

Subjects and methods

Participants

This study was approved by the King's College Hospital Research Ethics Committee (Ethics Ref 06/Q0703/124). After a full explanation of the methods involved, each subject gave written informed consent to take part in the study.

Twenty-eight participants diagnosed with juvenile myoclonic epilepsy (as determined by medical history, clinical features and EEG, as set by the International League Against Epilepsy) were identified using medical records (12 males, mean age: 34.07 years; see Table 1 for clinical details). Twelve patients (six males, mean age: 35.83 years) had experienced either myoclonic jerks or generalized tonic-clonic seizures within the 12 months before scanning. Thirty-eight healthy controls (17 males, mean age: 31.74 years) were recruited using a local volunteers' database. All control subjects took part in the DTI part of the study, but only 27 of these (12 males, mean age: 31.66 years) took part in the functional MRI phase of the study.

Image acquisition

All participants were scanned using a GE Signa 3 T HDx system based at the Centre for Neuroimaging Sciences, with actively shielded magnetic field gradients (maximum amplitude, 40 mT/m). The scanner's body coil was used for radio frequency transmission, and the manufacturer's standard eight-channel head coil was used for signal reception.

Structural magnetic resonance imaging

An inversion recovery-prepared 3D spoiled gradient echo 'T_1 volume' scan was obtained with an image matrix of 256 × 256 × 196 voxels, giving an isotropic voxel size of 1.1 mm (echo time/repetition time/inversion time = 2.8/6.6/450 ms, flip angle 20°).

Diffusion-weighted magnetic resonance imaging

DTI data were acquired using a peripherally gated, doubly refocused, spin echo echo-planar-imaging sequence, from 60 contiguous slices (orientation parallel to the anterior–posterior commissure line) with 2.4 mm^3 isotropic voxels (echo time = 104.5 ms, effective repetition time varying between subjects 12–20 RR intervals). At each slice location, four images were acquired with no diffusion gradients applied, together with 32 diffusion-weighted images (diffusion weighting b-value = 1300 s/mm). An ASSET (parallel imaging) speed up factor of 2.0 was used.

Functional magnetic resonance imaging

A gradient echo echo-planar-imaging sequence was used for the functional MRI acquisition using the following parameters: echo time = 25 ms, repetition time = 2500 ms, 50 interleaved 2.4 mm slices with a 0.1 mm interslice gap, an orientation parallel to the anterior–posterior commissure line, and a 64 × 64 matrix size over a 24 cm field of view giving a 3.75 mm in-plane voxel size. The excitation flip angle was 70°. An ASSET (parallel imaging) speed up factor of 2.0 was again used.

Image processing and statistical testing

Analyses reported here were conducted using a combination of tools from the FMRIB software library (FSL) (Smith *et al.*, 2004a, http://www.fmrib.ox.ac.uk/fsl), SPM8 (Wellcome Trust Centre for Neuroimaging, London, England, http://www.fil.ion.ucl.ac.uk/spm) and nipy (Millman and Brett, 2007, http://nipy.sourceforge.net) software toolkits.

Table 1 Demographics and clinical details of the patients with juvenile myoclonic epilepsy patients included in this study

Gender	Age	Age of onset	Myoclonic jerks per month	GTCS[a] per month	Recent seizure <1 year	Pharmacotherapy[b]
Male	22	16	1	0	Y	LEV 2000, VPA 2000
Female	26	15	15	0.3	Y	VPA 400, LMT 200, ZNS 400
Female	45	7	0	0.1	Y	LEV 1000, VPA 800
Male	49	20	0	0	N	LEV 1000, LMT 100, VPA 2000
Female	39	12	100	0	Y	VPA 400, LMT 450
Male	36	Teens	0	0	N	VPA 600
Female	64	20	0	0	N	LEV 2000
Female	25	15	0	0	N	LMT 200
Male	25	11	0	0	N	VPA 2400, LMT 300, ZNS 450
Female	41	17	0	0	Y	PHT 300 mg nocte, Metformine, Glucocide
Female	39	13	0	0	N	LEV 1000, VPA 1000
Female	22	14	4	0.4	Y	LEV 1500, LMT 600
Female	18	14	Unknown	Unknown	Unknown	LEV 1000, VPA 1000
Female	41	11	0.1	0	Y	VPA 800, LEV 1000, CLB prn
Female	29	15	0	0	N	VPA 2200, CLN 1 mg prn
Female	27	16	600	4	Y	OXC 2100, CLB 25
Male	40	16	0	0	N	LMT 300
Male	49	14	1	0.2	Y	LEV 2000, VPA 800
Male	36	16	0	0	N	VPA 2000, LMT 150
Male	29	16	0	0	N	None for 1 year, had LEV before
Male	35	19	0	0	N	VPA 1000
Male	25	16	4	1	Y	VPA 2000, LEV 1500
Female	32	Teens	10	1	Y	VPA 2000, CLB (as required)
Male	25	Teens	0	0	N	VPA 600
Female	32	16	0	0	N	VPA 200, LMT 400
Female	30	13	0	0	N	LMT 400, LEV 250
Male	32	13	0.1	0.1	Y	VPA 2000, LMT 400, LEV 500
Male	32	16	0	0	N	VPA 2000

CLB = clobazam; CLN = clonazepam; GTCS = generalized tonic clonic seizures; LEV = levetiracetam; LMT = lamotrigine; PHT = phenytoin; prn = *pro re nata*; VPA = valproate.

Diffusion-weighted magnetic resonance imaging

Preprocessing

Diffusion-weighted images were corrected for the effects of eddy-current–induced distortion and subject inter-scan motion, using in-house software based around eddy_correct (FSL); all images were realigned using an affine transformation to the initial image collected without diffusion weighting. Fitting the diffusion tensor to the eddy-corrected masked data using dtifit (FSL) created fractional anisotropy images. All subjects' fractional anisotropy data were then non-linearly registered to the standard fractional anisotropy template in Montreal Neurological Institute (MNI), distributed with the FSL package, using the non-linear registration tool FNIRT (Andersson *et al*., 2007).

Probabilistic tractography

BedpostX/ProbtrackX (Behrens *et al*., 2003) was used to prepare data for and perform probabilistic tractography. Up to two fibre populations were modelled per voxel. ProbtrackX was used to carry out the tractography, which was undertaken from each of 3440 voxels of the bilateral thalami as identified from the Harvard-Oxford subcortical atlas. In this step, 5000 streamlines were followed from each thalamic seed voxel, resulting in a 3D volume 'tractogram' representative of the spatial connection probability of that thalamic voxel. Exclusion masks were set at the brainstem (to focus on thalamo–cortical tracks) and the midline (to preclude artefactual streamlines crossing the corpus callosum). As masks were specified in MNI standard space, the non-linear transformations calculated in the previous step were used to perform the tractography in native space but the resulting tractograms were output in MNI space with a 2-mm isotropic voxel size. To reduce computational load at later processing stages, these images were then down-sampled from 2 to 3 mm isotropic voxel size.

To account for interindividual anatomical variation and misregistration, and to reduce noise, the resulting tractograms were spatially smoothed. Tractograms were smoothed by becoming Gaussian weighted averages of their immediate 26 neighbours in seed voxel space, analogous to temporal filtering in a time series. A full-width half-maximum Gaussian kernel of 4 mm was applied in seed space, meaning a tractogram from a given seed voxel became a weighted average of tractograms from neighbouring seed voxels. The resulting 3D images were then concatenated into two 4D volumes per subject representing tractograms for the left and right thalami, respectively.

Thalamic tractography parcellation

Thalamocortical bundles were parcellated using independent component analysis (Beckmann and Smith, 2005), a blind source separation technique that allows a parcellation of the thalamo–cortical white

matter bundles and identifies their thalamic origin (O'Muircheartaigh *et al.*, 2011*b*). The tensorial extension of independent component analysis (Beckmann and Smith, 2005) was implemented in the program Melodic (FSL). This adds 'subject' to the 'space' and 'time' domains, to allow for investigations of groups of subjects. In the context of this analysis, each volume in the 4D image represents the probabilistic tractogram from one thalamic seed voxel; it may be useful to consider the analogy of the more common application of tensorial independent component analysis to the analysis of functional time series, in which each volume reflects time-varying signals. Both the thalamic origin and its spatial connectivity are constrained to be consistent across subjects. Bayesian information criterion was used to automatically estimate the dimensionality of the decomposition, and the resulting component *z*-maps were thresholded using mixture modelling at $P > 0.5$. In addition, for every calculated component, the contribution of each subject to that component is output (subject mode).

The subject modes resulting from the decomposition represent the mean probabilistic tractography connectivity from the voxels in the thalamus that contribute to the independent component and, in this context, represent per-subject per-component connectivity between the thalamic regions and cortical targets. These were compared as in Damoiseaux *et al*. (2008). A general linear model was created using Glm (FSL), modelling for group membership, age and gender. Differences between groups were assessed by permutation using Randomise (FSL). Differences were considered significant at $P < 0.05$ (Bonferroni corrected for multiple comparisons) and trend at $P < 0.05$ (uncorrected for multiple comparisons).

Functional magnetic resonance imaging and clinical/psychological correlations

Behavioural data

The Controlled Oral Word Association Test (Loonstra *et al*., 2001), a standardized measure of phonemic fluency, was performed before functional MRI acquisition. Participants were asked to produce as many words as possible, beginning with a given letter, within 60 s. There were three trials; the first involved the letter 'F', the second the letter 'A' and the third the letter 'S'.

Functional magnetic resonance imaging task

An adaptation of the phonemic fluency task was performed during functional MRI acquisition. Participants were asked to subvocally generate words starting with a presented letter. The same letter was presented 10 times over 30 s in a block design. Participants were asked to try their best to match a word to every presentation of the letter. This was alternated with 30 s of passive viewing of an on-screen asterisk, also presented 10 times over 30 s. Participants were instructed to simply rest with eyes open during this period.

Preprocessing

Data were corrected for temporal slice-timing differences and inter-scan motion in one step using realign4D, provided in nipy (Roche *et al*., 2010). The time series was then high-pass filtered at 100 s to remove slow drifts from the data. A single volume was extracted from the middle of the time series to which the T_1 volume image was co-registered. This image was segmented into grey matter, white matter and CSF in SPM8 using the unified segmentation approach, which simultaneously calculates a transformation to standard MNI space (Ashburner and Friston, 2005). The resulting transformation from structural to MNI space was applied to the time series. Finally, data were smoothed using a 6-mm full-width at half-maximum Gaussian kernel.

Psychophysiological interaction

From the thalamic region of difference detected in the DTI analysis, the average time series was extracted from the unsmoothed functional data (to minimize signal bleed from the surrounding white matter structures). For each subject and session, a general linear model was formed representing the 30 s blocks of word generation—convolved with the canonical haemodynamic response function—representing the task, the raw thalamic time series (allowing testing of functional connectivity between the thalamus and the rest of the brain) and the interaction of the two. The interaction term (where non-zero) represents a task-modulated change in functional connectivity, or psychophysiological interaction (Friston *et al*., 1997). In addition, a series of six motion parameters and the mean time series from white matter and CSF areas (using white matter and CSF probability maps output as part of unified segmentation) were used as confound regressors. These data were modelled using the FSL package Flame (Smith *et al*., 2004*a*).

Group comparison of psychophysiological interaction

The single-subject results of the psychophysiological interaction analysis were fed into a higher-level mixed effects model, estimated using Flame with outlier deweighting (Woolrich, 2008; FSL). Here we modelled the average effect of task, functional connectivity and psychophysiological interaction in healthy controls, as well as the contrast of psychophysiological interaction between groups. Images were thresholded with clusters determined at $P < 0.01$, and a cluster significance level of $P < 0.05$, corrected for multiple comparisons.

Post hoc clinical correlations

Patients were divided into those with recent seizure activity (in the 12 months before scanning) and those who were in remission. This was to accommodate an analysis investigating the relationship of seizure activity with MRI-derived variables.

From the DTI data, subject modes were extracted from thalamic DTI bundles that showed significantly different connectivity. From the functional MRI data, parameter estimates (betas) were extracted from areas of significantly different psychophysiological interaction activity. Where appropriate, Pearson- or Spearman-rank correlations were carried out between these DTI thalamo–cortical connectivity and psychophysiological interaction differences and (i) duration of epilepsy in years; (ii) number of myoclonic jerks per month; (iii) number of generalized tonic-clonic seizures per month and (iv) performance on phonemic fluency. Significant correlations are reported at $P < 0.05$ (Bonferroni corrected for multiple comparisons) or trend at $P < 0.05$ (uncorrected).

Results

Thalamic diffusion tensor imaging connectivity

The number of components for each thalamus was automatically estimated using Bayesian information criteria. Fourteen left and 15 right spatial thalamic components were estimated using probabilistic independent component analysis. The resulting components showed a similar spatial distribution to those in our previous study

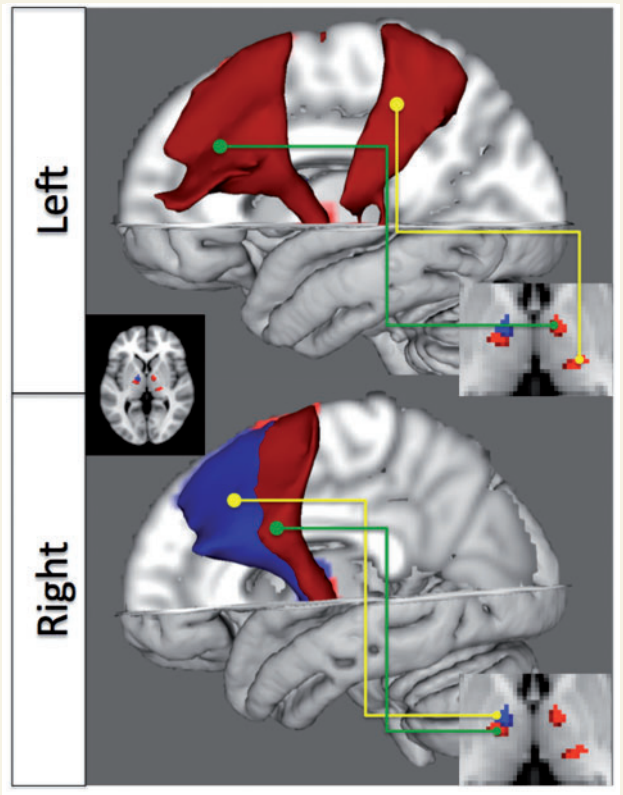

Figure 1 Thalamo–cortical bundles showing reduced tractography-defined connectivity between normal subjects and patients with juvenile myoclonic epilepsy (blue, $P < 0.05$, corrected for multiple comparisons; red, $P < 0.05$, uncorrected) relative to healthy controls. Images on the *right* show the regions in the thalamus from which the bundles originate.

of normal subjects (O'Muircheartaigh *et al.*, 2011*b*). Moreover, the spatial distribution was similar across subjects (see Supplementary Fig. 1 for single subject results of tractography seeded from the thalamic region illustrated in red in Fig. 1).

A single component in the right anterior thalamic projection to the SMA survived Bonferroni multiple testing correction (29 tests, $P < 0.05$), showing significantly decreased probability of connection in patients with juvenile myoclonic epilepsy. This region lies in the ventral anterior/ventral lateral groups of thalamic nuclei, regions with strong functional and anatomical correspondence with the SMA, pre-SMA and motor cortex (McFarland and Haber, 2002). This is reflected spatially by the course of the bundle in Fig. 1. A further right-sided bundle and two left-sided bundles were detected at trend level of significance ($P < 0.05$ uncorrected). Of these, there is striking spatial correspondence between the left anterior bundle and the statistically significant right-sided bundle.

Functional magnetic resonance imaging results

Task-activated regions for the covert verbal fluency task (Fig. 2A) were similar to comparable studies in healthy controls (e.g. Allen and Fong, 2008), with activation in the SMA, bilateral inferior frontal gyrus with a leftward emphasis, left premotor area, left thalamus and bilateral putamina, as well as bilateral ventral visual areas. Functional connectivity with the thalamic region (Fig. 2B and C) also corresponds to previously reported results (Fair *et al.*, 2010). The region of the thalamus showing altered structural connectivity in the DTI analysis had positive functional connectivity in both groups with premotor and SMA areas, as well as an extensive basal ganglial region, encompassing bilateral caudate, putamen and globus pallidus. This further strongly suggests that the thalamic region defined by the DTI analysis is functionally integrated with ventral anterior/lateral groups of thalamic nuclei. Negative connectivity was detected in bilateral motor/somatosensory cortex as well as a region of lateral occipital cortex, although only in the controls. This connectivity was not significant in the patient group.

There was a significant psychophysiological interaction between the thalamic region and bilateral SMA and cingulum, as well as right-sided dorsolateral prefrontal cortex and lateral parietal cortex (Fig. 2D). Anterior right-sided thalamus functional connectivity to these regions was significantly modulated by verbal fluency performance, as measured before the scanning session, and task performance was associated with reduced activity.

No group differences were detected between groups for the task condition or for functional connectivity. A two-sided *t*-test contrast comparing psychophysiological interaction in healthy controls and patients with juvenile myoclonic epilepsy showed significant ($P < 0.05$ corrected for multiple comparisons using cluster extent) differences in psychophysiological interaction in right superior frontal cortex (Fig. 3). Participants with juvenile myoclonic epilepsy showed increased task-dependent functional connectivity with frontal cortex relative to controls.

Post hoc clinical anatomical correlations

Two variables (number of generalized seizures in the last year, and duration of illness in years) and their log transformations were significantly non-normally distributed, so correlations involving these variables used Spearman rank correlations. For all other variables, reported correlations are Pearson. Performance on the phonemic verbal fluency task before the scan showed a positive trend with psychophysiological interaction betas in those with active juvenile myoclonic epilepsy ($r = 0.587$, $df = 12$, $P < 0.05$, uncorrected), and a significant negative relationship in those with juvenile myoclonic epilepsy in remission ($r = -0.655$, $df = 16$, $P < 0.05$, corrected). Furthermore, there was a positive trend between psychophysiological interaction betas and the number of generalized seizures in the previous year ($r = 0.579$, $df = 12$, $P < 0.05$, uncorrected). The relationship between number of generalized seizures and verbal fluency score was non-significant ($r = 0.107$, $df = 12$, $P > 0.74$).

Post hoc regression of structural connectivity on task-modulated functional connectivity

Functional connectivity between the thalamus and bilateral hippocampi, left putamen and bilateral globus pallidus became more

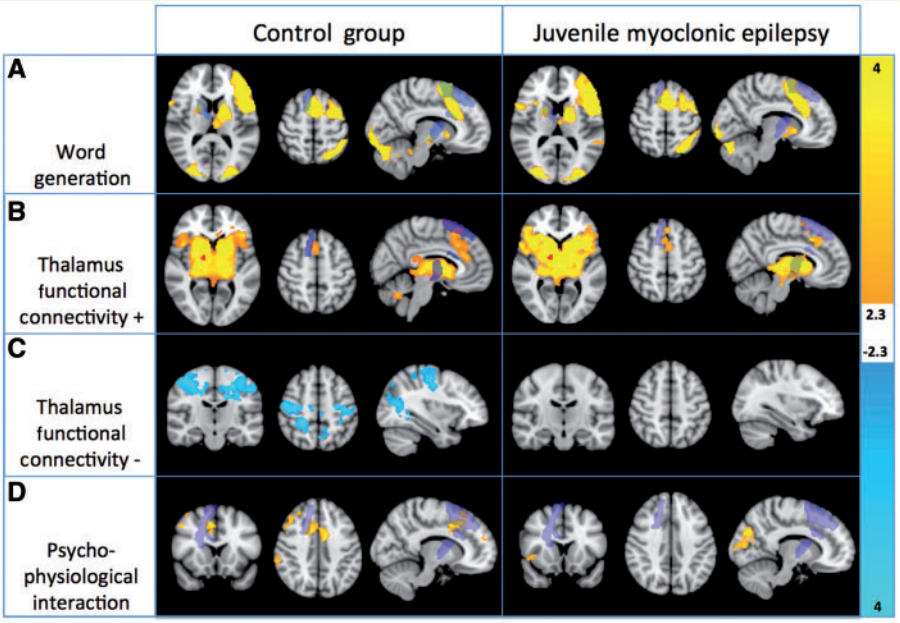

Figure 2 Group average results for each group for the word generation task (**A**), positive (**B**) and negative (**C**) correlation with the thalamic seed region, and psychophysiological interaction between the thalamic seed time series and the task (**D**). This interaction is negative, i.e. functional connectivity decreases as a function of task performance. All results are presented $P < 0.05$, corrected for multiple comparisons. The thalamic bundle defined by the DTI analysis is overlaid in purple.

strongly negative with increasing thalamo–cortical structural connectivity from the DTI analysis. Task-modulated activity (psychophysiological interaction) in the anterior cingulate as well as bilateral putamina and globus pallidus showed a strong positive relationship with structural thalamo–cortical connectivity from the right thalamus.

Discussion

The multimodal MRI data described here provide anatomically specific evidence for the involvement of thalamus in juvenile myoclonic epilepsy. The reduction in connectivity from the thalamus to the SMA/premotor region indicates a structural alteration of the thalamo–cortical motor control circuit as described by Alexander and Crutcher (1990) and that the thalamic region is involved in abnormal and increased cognition-modulated functional coherence with anterior frontal and premotor cortex. This task-modulated connectivity is increased in those with frequent seizures. Finally, the strength of structural connectivity relates to increasing task-driven functional connectivity in the putamen in patients. In combination, these data provide a network model of seizure activity and neuropsychological dysfunction in juvenile myoclonic epilepsy.

The novel approach used linked structural connectivity with functional connectivity and effective connectivity. The methods include both data driven (the structural segmentation of the thalamus) and hypothesis driven (the verbal fluency task) approaches. We segmented the thalamus based on connectivity without the need of predefined regions of interest that may bias results. The identified tract origins were used as seeds in the functional and psychophysiological interaction, ensuring the regions of interest were anatomically meaningful, another potential source of bias in functional connectivity analyses (Smith *et al.*, 2011). Finally, using prior knowledge of cognitive dysfunction in this group (O'Muircheartaigh *et al.*, 2011*a*), we interrogate changes in thalamo–cortical functional integration from this region of interest to the rest of the brain.

Alterations in structural connectivity

The comparison of thalamic DTI-based connectivity using the novel independent component analysis-DTI approach extends the previous findings of reduced fractional anisotropy within a region of the left anterior thalamus (Deppe *et al.*, 2008). Although fractional anisotropy correlated with frequency of generalized tonic-clonic seizures, this study investigated a restricted region of interest in the anterior thalamus. Fractional anisotropy is a summary and non-specific measure, and changes thereof may relate to many effects, including crossing fibres in a voxel (Jbabdi *et al.*, 2010) and partial volume effects; the area of significant changes is also highly dependent on the choice of spatial filtering (e.g. Jones *et al.*, 2005). We used a weighted measure of structural connectivity from the thalamic voxels within the white matter bundle identified. This avoids some of the previous confounds as (i) multiple fibres are modelled in this implementation of probabilistic tractography (Behrens *et al.*, 2003); and (ii) spatial filtering occurs in seed space. This technique is conceptually more similar to anatomical connectivity mapping (Bozzali *et al.*, 2010) or track-density imaging (Calamante *et al.*, 2010), although providing tract-specific measurements; it needs less prior anatomical

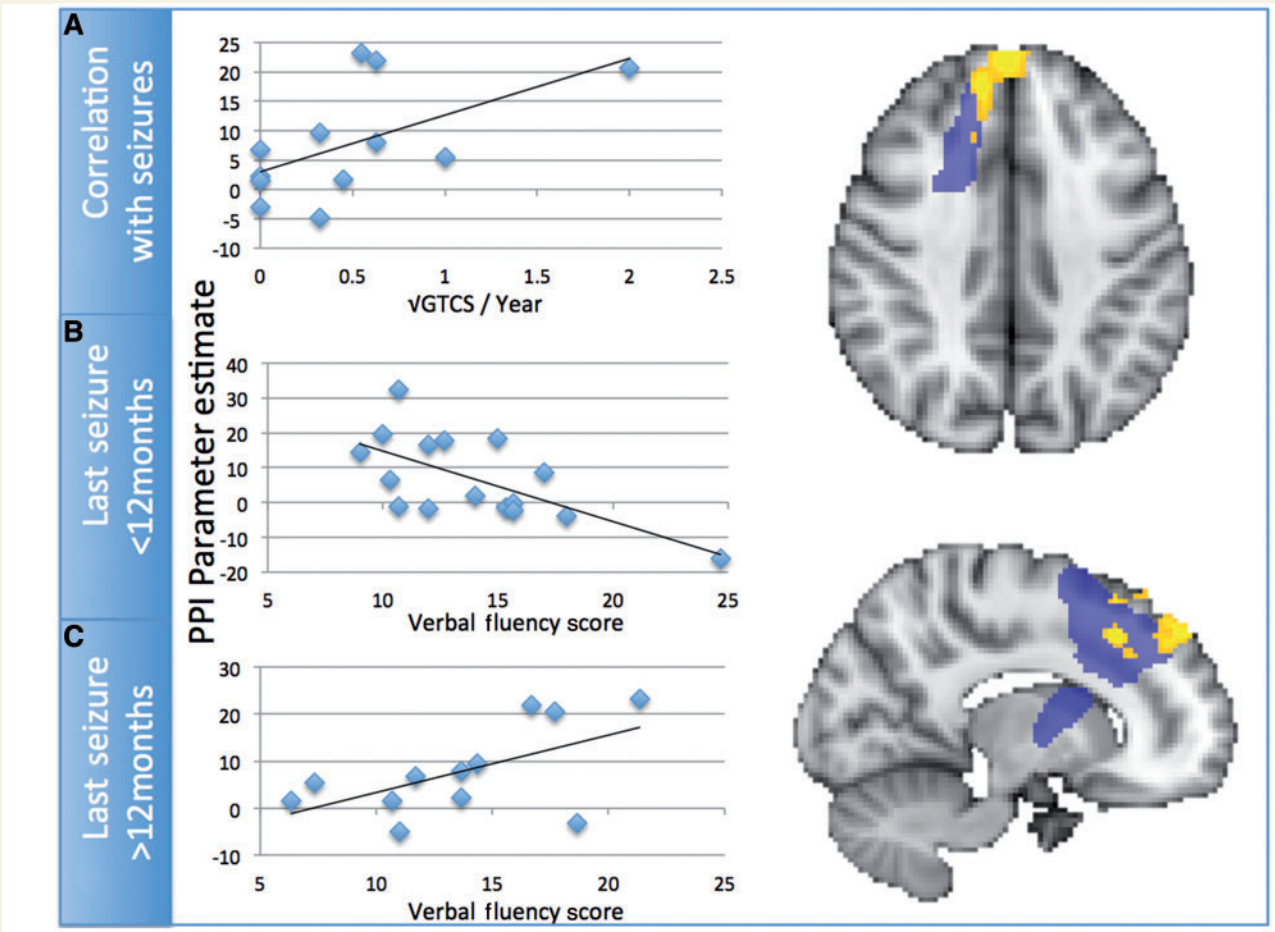

Figure 3 (**A**) Differential psychophysiological interaction between healthy controls and patients with juvenile myoclonic epilepsy. Patients with juvenile myoclonic epilepsy show increased psychophysiological interaction with the thalamic seed region. Psychophysiological interaction in patients with active juvenile myoclonic epilepsy correlated significantly with the number of generalized tonic clonic seizures in the previous year. (**B** and **C**) The relationship between performance on the verbal fluency test and psychophysiological interaction in the mesial pre-SMA region. There is an interaction in this relationship dependent on disease status in the juvenile myoclonic epilepsy group. GTCS = general tonic-clonic seizures.

hypotheses compared with standard region of interest tractography, reducing subjective bias.

Task-modulated functional connectivity

Thalamocortical functional connectivity to right-sided medial prefrontal, lateral prefrontal and lateral parietal regions was reduced in response to the verbal fluency task in healthy controls, indicating a modulating influence by the thalamic region. However, this effect was absent in the patients with juvenile myoclonic epilepsy in the medial frontal region, indicating a relative failure of this thalamic region to reduce premotor activity. This was strongly related to performance in this group, but this relationship was dependent on whether the epilepsy was in remission or not. The degree of thalamo–cortical functional connectivity (with higher levels of connectivity representing abnormality compared with controls) increased with seizure frequency.

In concurrent EEG–functional MRI studies of mixed groups of patients with idiopathic generalized epilepsy, generalized spike and wave discharges have been shown to be correlated with increased blood oxygen level–dependent activity in cortex and decreased thalamic blood oxygen level–dependent activity (Gotman *et al*., 2005; Hamandi *et al*., 2006). Compared with other idiopathic generalized epilepsies, juvenile myoclonic epilepsy commonly involves multiple spikes at a higher frequency than in childhood absence epilepsy (Holmes *et al*., 2010). Despite the differences in morphology of generalized spike and wave in juvenile myoclonic compared with childhood absence epilepsy, modelling studies show that the same thalamo–cortical network substrate is capable of generating the faster polyspike generalized spike and wave of juvenile myoclonic epilepsy as well as the slower generalized spike and wave of other idiopathic generalized epilepsies (Marten *et al*., 2009; Rodrigues *et al*., 2009). This may be due to differential modulatory influences of the subcortical and cortical structures involved.

Basal ganglia, thalamus and cortex

The anatomical specificity of the structural and functional results to known basal ganglia circuits is striking. Although the spatial

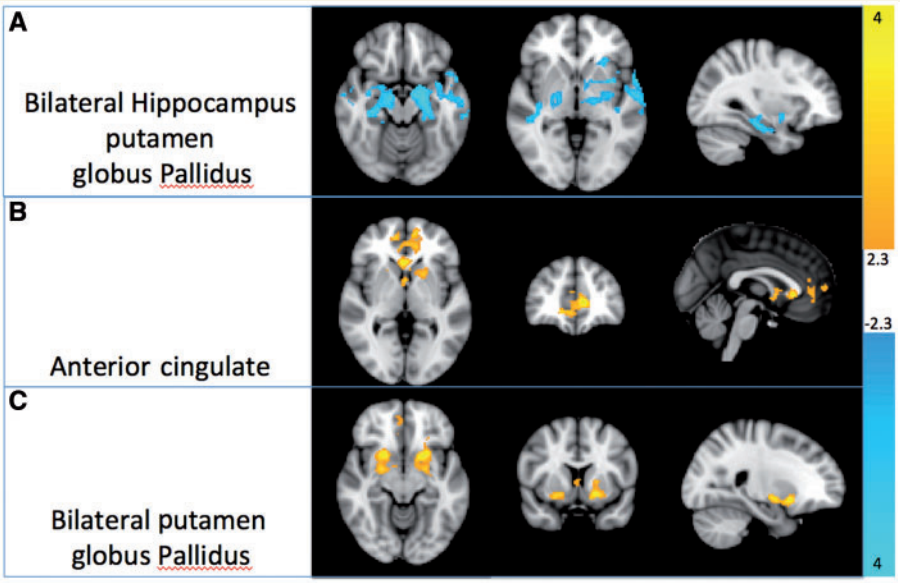

Figure 4 (**A**) Decreasing thalamo–cortical structural connectivity with the SMA is associated with increased thalamic functional connectivity to subcortical structures including hippocampus, amydala, putamen and globus pallidus. Reduced structural thalamo–cortical connectivity is associated with reduced co-activity within the thalamus and anterior cingulate (**B**) and bilateral basal ganglia regions (**C**).

localization of techniques such as DTI and functional MRI are limited, both the thalamo–cortical bundle and its thalamic origin match with known connections from tracer studies (McFarland and Haber, 2002). The raw functional connectivity results (Fig. 2B and C) accord with the subcortical-cortical motor circuit (Alexander and Crutcher, 1990) of SMA and motor cortex connectivity. This is emphasized by the linear relationship between structural connectivity, as measured here using DTI, and task-modulated functional connectivity in bilateral putamen and globus pallidus (Fig. 4), critical basal ganglia structures for this circuit. The ventrolateral nuclei of the thalamus act as a relay for motor signals from the striatum to cortex, but also feedback to the striatum (Smith *et al*., 2004*b*). This increasing functional connectivity between thalamus and striatum may be a function of this feedback, or of the larger scale thalamus to cortex to striatum loop.

The anatomical circuit described is not a simple motor input or output circuit. Of particular relevance to juvenile myoclonic epilepsy is the role of basal ganglia loops in executive and attentional function (Brown and Marsden, 1998). In this context, the disruption of a basal ganglia–thalamo–cortical loop associates intuitively with changes in executive behaviour in juvenile myoclonic epilepsy (Piazzini *et al*., 2008; Pulsipher *et al*., 2009; O'Muircheartaigh *et al*., 2011a). Moreover, the same loops are implicated as anatomical correlates of myoclonus (Richardson *et al*., 2006). Neurochemical studies using PET have indicated specific dopamine-binding reduction in substantia nigra and midbrain (Ciumas *et al*., 2008) and bilateral putamen (Landvogt *et al*., 2010). These regions also provide input to the circuit (Alexander and Crutcher, 1990). Our data outline the specific anatomical and functional anatomy of both the characteristic myoclonic jerks and the neuropsychological deficits seen in juvenile myoclonic epilepsy.

We have previously demonstrated changes in functional and structural connectivity between the SMA and motor cortex during a working memory task (Vollmar *et al*., 2011, 2012) and related them to changes in cortico-cortical structural connectivity. The data presented here may further clarify the mechanisms of this increased connectivity, via decreased thalamic inhibition of the SMA and premotor cortex. The current study design, however, was not optimal for separating out the directionality of functional and structural changes, and a longitudinal study would be more appropriate. In such a study, Pulsipher *et al.* (2011) demonstrated a faster rate of thalamic volume loss in a mixed paediatric group of patients with idiopathic generalized epilepsy compared with healthy children, although their volumes were not significantly different on diagnosis. This may indicate that the functional changes (in this case, seizures) precede the structural changes. Even without knowing the directionality of the changes, we can conclude that there is a dissociation between structural thalamo–cortical brain changes in juvenile myoclonic epilepsy, along with aberrant functional thalamo–cortical interactions that get worse as a function of disease severity as generalized tonic clonic seizures relate to more severe task-related dysfunction (Fig. 3A).

In conclusion, there have been many findings of neuropsychological and executive dysfunction in juvenile myoclonic epilepsy. However, there has been a significant variability of structural magnetic resonance data, with abnormalities reported in thalami (Bernhardt *et al*., 2009; Pulsipher *et al*., 2009, 2011; Du *et al*., 2011; Keller *et al*., 2012), putamen (Keller *et al*., 2011) and cortex (Woermann *et al*., 1998; Betting *et al*., 2006; Kim *et al,* 2007; O'Muircheartaigh *et al*., 2011a). Our results provide an integrated framework that may help to elucidate previously disparate findings.

We emphasize the role of the basal ganglia motor loop in the disease process of juvenile myoclonic epilepsy and the associated

neuropsychological impairments. The reductions of structural and functional connectivity of this region to the superior frontal and SMA regions implicate a specific thalamo–cortical network dysfunction. The genetic aetiology of juvenile myoclonic epilepsy is likely to be heterogeneous and complex (Zifkin *et al*., 2005) but the phenotypic expression is consistent. Our findings support the concept of idiopathic epilepsies as system disorders (Avanzini *et al*., 2012). If these results are specific to juvenile myoclonic epilepsy, studies of structural and functional connectivity may help elucidate the pathophysiology of generalized epilepsies.

Funding

We are grateful to the Wellcome Trust for supporting our work (Project Grant No 079474), and the authors acknowledge infrastructure support from the National Institute for Health Research Specialist Biomedical Research Centre for Mental Health at the South London and Maudsley NHS Foundation Trust and the Institute of Psychiatry, King's College London. Part of this work was undertaken at University College London Hospitals who received a proportion of funding from the National Institute for Health Research, Biomedical Research Centres funding scheme. J.O.M. is supported by a Sir Henry Wellcome Postdoctoral Fellowship awarded by the Wellcome Trust (No 096195).

Supplementary material

Supplementary material is available at *Brain* online.

References

Aghakhani Y, Bagshaw AP, Benar CG, Hawco C, Andermann F, Dubeau F, et al. fMRI activation during spike and wave discharges in idiopathic generalized epilepsy. Brain 2004; 127: 1127–44.

Alexander GE, Crutcher MD. Functional architecture of basal ganglia circuits: neural substrates of parallel processing. Trends Neurosci 1990; 13: 266–71.

Allen MD, Fong AK. Clinical application of standardized cognitive assessment using fMRI. II. Verbal fluency. Behav Neurol 2008; 20: 141–52.

Andersson JLR, Jenkinson M, Smith SM. Nonlinear registration, aka Spatial normalisation. FMRIB Technical Report TR07JA2, FMRIB Analysis Group of the University of Oxford, 2007. www.fmrib.ox.ac.uk/analysis/techrep.

Ashburner J, Friston KJ. Unified segmentation. NeuroImage 2005; 26: 839–51.

Avanzini G, Manganotti P, Meletti S, Moshé SL, Panzica F, Wolf P, et al. The system epilepsies: a pathophysiological hypothesis. Epilepsia 2012; 53: 771–8.

Beckmann C, Smith SM. Tensorial extensions of independent component analysis for multisubject FMRI analysis. NeuroImage 2005; 25: 294–311.

Behrens TEJ, Woolrich MW, Jenkinson M, Johansen-Berg H, Nunes RG, Clare S, et al. Characterization and propagation of uncertainty in diffusion-weighted MR imaging. Magn Reson Med 2003; 50: 1077–88.

Bernhardt BC, Rozen DA, Worsley KJ, Evans AC, Bernasconi N, Bernasconi A. Thalamo-cortical network pathology in idiopathic generalized epilepsy: insights from MRI-based morphometric correlation analysis. Neuroimage 2009; 46: 373–81.

Betting LE, Mory SB, Li LM, Lopes-Cendes I, Guerreiro MM, Guerreiro CAM, et al. Voxel-based morphometry in patients with idiopathic generalized epilepsies. Neuroimage 2006; 32: 498–502.

Blumenfeld H. From molecules to networks: cortical/subcortical interactions in the pathophysiology of idiopathic generalized epilepsy. Epilepsia 2003; 44: 7–15.

Bozzali M, Parker GJ, Serra L, Embleton K, Gill T, Perri R, et al. Anatomical connectivity mapping: a new tool to assess brain disconnection in Alzheimer's disease. Neuroimage 2010; 54: 2045–51.

Brown P, Marsden CD. What do the basal ganglia do. The Lancet 1998; 351: 1801–4.

Calamante F, Tournier JD, Jackson GD, Connelly A. Track-density imaging (TDI): super-resolution white matter imaging using whole-brain track-density mapping. Neuroimage 2010; 53: 1233–43.

Ciumas C, Wahlin TB, Jucaite A, Lindstrom P, Halldin C, Savic I. Reduced dopamine transporter binding in patients with juvenile myoclonic epilepsy. Neurology 2008; 9: 788–94.

da Silva Sousa P, Lin K, Garzon E, Ceiki Sakamoto A, Yacubian EM. Language- and praxis-induced jerks in patients with juvenile myoclonic epilepsy. Epileptic Disord 2005; 7: 115–21.

Damoiseaux JS, Beckmann CF, Sanz Arigita EJ, Barkhof F, Scheltens P, Stam CJ, et al. Reduced resting-state brain activity in the "default network" in normal aging. Cereb Cortex 2008; 18: 1856–64.

Danober L, Deransart C, Depaulis A, Vergnes M, Marescaux C. Pathophysiological mechanisms of genetic absence epilepsy in the rat. Prog Neurobiol 1998; 55: 27–57.

Deppe M, Kellinghaus C, Duning T, Moddel G, Mohammadi S, Deppe K, et al. Nerve fiber impairment of anterior thalamo-cortical circuitry in juvenile myoclonic epilepsy. Neurology 2008; 71: 1981–5.

Du H, Zhang Y, Xie B, Wu N, Wu G, Wang J, et al. Regional atrophy of the basal ganglia and thalamus in idiopathic generalized epilepsy. J Magn Reson Imaging 2011; 33: 817–21.

Fair DA, Bathula D, Mills KL, Dias TGC, Blythe MS, Zhang D, et al. Maturing thalamo-cortical functional connectivity across development. Front Syst Neurosci 2010; 4: 10. doi:10.3389/fnsys.2010.00010.

Friston KJ, Buchel C, Fink GR, Morris J, Rolls E, Dolan R. Psychophysiological and modulatory interactions in Neuroimaging. NeuroImage 1997; 6: 218–29.

Genton P, Gelisse P. Juvenile myoclonic epilepsy. Arch Neurol-Chicago 2001; 8: 1487–90.

Gotman J, Grova C, Bagshaw A, Kobayashi E, Aghakhani Y, Dubeau F. Generalized epileptic discharges show thalamo-cortical activation and suspension of the default state of the brain. Proc Natl Acad Sci USA 2005; 102: 15236–40.

Hamandi K, Salek-Haddadi A, Laufs H, Liston A, Friston K, Fish DR, et al. EEG-fMRI of idiopathic and secondarily generalized epilepsies. Neuroimage 2006; 31: 1700–10.

Holmes MD, Quiring J, Tucker DM. Evidence that juvenile myoclonic epilepsy is a disorder of frontotemporal corticothalamic networks. Neuroimage 2010; 49: 80–93.

Janz D. Epilepsy with impulsive petit mal (juvenile myoclonic epilepsy). Acta Neurol Scand 1985; 72: 449–59.

Jbabdi S, Behrens TE, Smith SM. Crossing fibres in tract-based spatial statistics. Neuroimage 2010; 49: 249–56.

Jones DK, Symms MR, Cercignani M, Howard RJ. The effect of filter size on VBM analyses of DT-MRI data. Neuroimage 2005; 26: 546–54.

Keller SS, Ahrens T, Mohammadi S, Möddel G, Kugel H, Bernd Ringelstein E, et al. Microstructural and volumetric abnormalities of the putamen in juvenile myoclonic epilepsy. Epilepsia 2011; 52: 1715–24.

Kim JH, Lee JK, Koh S, Lee S-A, Lee J-M, Kim SI, et al. Regional grey matter abnormalities in juvenile myoclonic epilepsy: a voxel-based morphometry study. Neuroimage 2007; 37: 1132–7.

Keller SS, Gerdes JS, Mohammadi S, Kellinghaus C, Kugel H, Deppe K, et al. Volume estimation of the thalamus using FreeSurfer and Stereology on MR images: consistency between methods. Neuroinformatics 2012; 10: 341–50.

Krause M, Mahant N, Kotschet K, Fung VS, Vagg D, Wong CH, et al. Dysexecutive behaviour following deep brain lesions—a different type of disconnection syndrome? Cortex 2012; 48: 97–119.

Landvogt C, Buchholz HG, Bernedo V, Schreckenberger M, Werhahn KJ. Alterations of dopamine D2/D3 receptor binding in patients with juvenile myoclonic epilepsy. Epilepsia 2010; 51: 1699–706.

Loonstra AS, Tarlow AR, Sellers AH. COWAT metanorms across age, education, and gender. Appl Neuropsychol 2001; 8: 161–6.

Marten F, Rodrigues S, Benjamin O, Richardson MP, Terry JR. Onset of polyspike complexes in a mean-field model of human electroencephalography and its application to absence epilepsy. Phil Trans R Soc A 2009; 367: 1145–61.

McFarland NR, Haber SN. Thalamic relay nuclei of the basal ganglia form both reciprocal and nonreciprocal cortical connections, linking multiple frontal cortical areas. J Neurosci 2002; 22: 8117–32.

Millman KJ, Brett M. Analysis of functional magnetic resonance imaging in Python. Computing in Science and Engineering 2007; 9: 52–5.

Montalenti E, Imperiale D, Rovera A, Bergamasco B, Benna P. Clinical features, EEG findings and diagnostic pitfalls in juvenile myoclonic epilepsy: a series of 63 patients. J Neurol Sci 2001; 184: 65–70.

O'Muircheartaigh J, Vollmar C, Barker G, Kumari V, Symms M, Thompson P, et al. Focal structural changes and cognitive dysfunction in juvenile myoclonic epilepsy. Neurology 2011a; 76: 34–40.

O'Muircheartaigh J, Vollmar C, Traynor C, Barker GJ, Kumari V, Symms MR, et al. Clustering probabilistic tractograms using independent component analysis applied to the thalamus. NeuroImage 2011b; 54: 2020–32.

Piazzini A, Turner K, Vignoli A, Canger R, Canevini MP. Frontal cognitive dysfunction in juvenile myoclonic epilepsy. Epilepsia 2008; 49: 657–62.

Pulsipher DT, Dabbs K, Tuchsherer V, Sheth D, Koehn MA, Hermann P, et al. Thalamofrontal neurodevelopment in new-onset pediatric idiopathic generalized epilepsy. Neurology 2011; 76: 28–33.

Pulsipher DT, Seidenberg M, Guidotti L, Tuchscherer VN, Morton J, Sheth RD, et al. Thalamofrontal circuitry and executive dysfunction in recent-onset juvenile myoclonic epilepsy. Epilepsia 2009; 50: 1210–19.

Richardson MP, Grosse P, Allen PJ, Turner R, Brown P. BOLD correlates of EMG spectral density in cortical myoclonus: description of method and case report. Neuroimage 2006; 32: 558–65.

Roche A. A four-dimensional registration algorithm with application to joint correction of motion and slice timing in fMRI. IEEE Trans Med Imaging 2011; 30: 1546–54.

Rodrigues S, Barton D, Szalai R, Benjamin O, Richardson MP, Terry JR. Transitions to spike-wave oscillations and epileptic dynamics in a human cortico-thalamic mean-field model. J Comput Neurosci 2009; 27: 507–26.

Roebling R, Scheerer N, Uttner I, Grube O, Kraft E, Lerche H. Evaluation of cognition, structural, and functional MRI in juvenile myoclonic epilepsy. Epilepsia 2009; 50: 2456–65.

Smith SM, Jenkinson M, Woolrich MW, Beckmann CF, Behrens TEJ, Johansen-Berg H, et al. Advances in functional and structural MR image analysis and implementation as FSL. NeuroImage 2004a; 23: 208–19.

Smith SM, Miller KL, Salimi-Khorshidi G, Webster M, Beckmann CF, Nichols TE, et al. Network modelling methods for FMRI. Neuroimage 2011; 54: 875–91.

Smith Y, Raju D, Pare J-F, Sidibe M. The thalamostriatal system: a highly specific network of the basal ganglia circuitry. Trends Neurosci 2004b; 27: 520–7.

Vollmar C, O'Muircheartaigh J, Barker GJ, Symms MR, Thompson P, Kumari V, et al. Motor-cortex hyperconnectivity in juvenile myoclonic epilepsy—a cognitive fMRI study. Brain 2011; 134: 1710–19.

Vollmar C, O'Muircheartaigh J, Barker GJ, Symms MR, Thompson P, Kumari V, et al. Altered microstructural connectivity in juvenile myoclonic epilepsy: the missing link. Neurology 2012; 78: 1555–9.

Vulliemoz S, Vollmar C, Koepp MJ, Yogarajah M, O'Muircheartaigh J, Carmichael DW, et al. Connectivity of the supplementary motor area in juvenile myoclonic epilepsy and frontal lobe epilepsy. Epilepsia 2010; 52: 507–14.

Woermann FG, Sisodiya SM, Free SL, Duncan JS. Quantitative MRI in patients with idiopathic generalized epilepsy: evidence of widespread cerebral structural changes. Brain 1998; 121: 1661–7.

Woolrich M. Robust group analysis using outlier inference. Neuroimage 2008; 41: 286–301.

Zifkin B, Andermann E, Andermann F. Mechanisms, genetics, and pathogenesis of juvenile myoclonic epilepsy. Curr Opin Neurol 2005; 18: 147–53.